

Computational Engineering of the Stability and Optical Gaps of SiC Quantum Dots

Fernando A. Reboredo,^{*,†} Laurent Pizzagalli,[‡] and Giulia Galli[†]

Lawrence Livermore National Laboratory, Livermore, California 94551, and
Université de Poitiers, 86960 Futuroscope, Cedex, France

Received January 20, 2004

ABSTRACT

We have carried out an ab initio computational study of SiC nanoparticles with diameters between 1 and 3 nm. Our calculations show that surface composition and termination play a dominant role in determining the optical gaps and thermodynamic stability of these nanoparticles. In particular, we find that the optical gap of cubic SiC dots can be engineered as a function of their size and surface composition to obtain absorption and emission from the UV to the green. Our results suggest that SiC nanoparticles may be used to build new materials for semiconductor-based UV light sources.

Design and control of matter at the nanoscale hold great promises for the development of novel materials and devices with target properties, directly engineered from the quantum-mechanical behavior of electrons and ions.¹ Ab initio computational tools are playing an increasingly important role in achieving this degree of control, by describing and predicting with quantitative accuracy the property of materials based on their atomic and molecular constituents.²

In this letter, we present a series of ab initio calculations aimed at designing semiconductor nanostructures with specific optical properties. In particular, we consider the case of SiC dots and we propose that their stability and optical gaps can be engineered as a function of size, surface structure, and composition, so as to build materials for semiconductor-based ultraviolet (UV) light sources.

Silicon carbide is a wide band gap semiconductor, and it is a biocompatible material; therefore, SiC dots are good candidates for nanostructured labels of biological molecules and they are possibly superior to, e.g., Si nanoparticles, for their stability in oxygen atmosphere. Despite their potential technological applications and the fundamental interest in compound nanostructured materials, investigations of SiC quantum dots (QDs) are still in the early stages. Although several experimental studies have recently appeared, they have not yet been accompanied by theoretical investigations, so far limited to small clusters relevant to astrophysical studies³ or molecular dynamics simulations of the sintering of polycrystalline SiC.⁴

Synthesis of β -SiC QDs has been achieved by C⁺ implantation in bulk Si followed by subsequent etching,⁵ by implantation of C in SiO₂,⁶ or co-implantation of Si and C in zeolites.⁷ These techniques have yielded nanoparticles showing quantum confinement effects, e.g., emission above the bulk gap, which in SiC varies from 2 to 2.8 eV depending on the polytype. Moreover, β -SiC nanocrystals have been synthesized using CVD,⁸ pyrolysis,⁹ or direct etching of bulk β -SiC;¹⁰ however, the QDs obtained in this way were too large (\sim 10 nm) to show any quantum confinement. Finally, SiC dots have been obtained by etching hexagonal SiC(6H-SiC) crystals, yielding contradictory results on quantum confinement effects.^{11–13}

The observation of quantum confinement in SiC nanostructures opens the interesting possibility of designing materials with blue or higher frequency emission, e.g., UV. The development of semiconductor-based UV light sources—at present mostly limited to nitride compounds—is of critical importance to many new technologies ranging from the detection of biological agents and non-line-of-sight (NLOS) covert communications to water purification.

With the aim of engineering SiC dots with given optical gaps, we performed a series of ab initio calculations to study the interplay between quantum confinement effects and surface composition and structure in SiC nanoparticles with 1 to 3 nm diameter. Our results show that, irrespective of size, dots with hydrogenated, unreconstructed C-terminated surfaces and (2 \times 1)-reconstructed Si-terminated surfaces are the most stable, and, for the same diameter, they can have gaps differing as much as 1 to 1.5 eV. Interestingly, hydrogen rich, C-terminated SiC dots smaller than 2 nm have gaps

* Corresponding author.

[†] Lawrence Livermore National Laboratory.

[‡] Université de Poitiers.

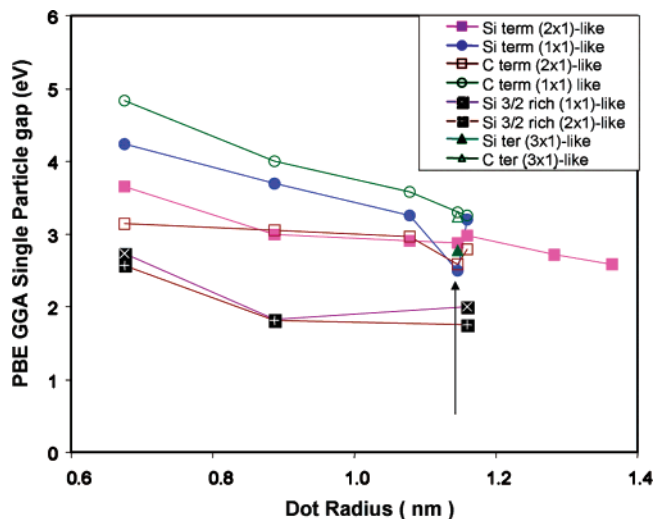


Figure 1. Single-particle electronic gap of SiC quantum dots as a function of size for different surface structures. The gap has been computed within the generalized gradient corrected approximation (GGA-PBE)¹⁴ (see text). The arrow indicates the dot sizes shown in Figure 2.

larger than those of C, Si, and Ge nanoparticles of the same size, and they are good candidates to be UV emitters.

Our ab initio calculations were performed using density functional theory within the gradient corrected approximation of Perdew, Burke, and Ernzerhof¹⁴ (PBE). We used a plane-wave pseudopotential method and the GP code.¹⁵ The Si and C pseudopotentials were generated with the Troullier–Martins prescription,¹⁶ and we used a kinetic energy cutoff of 35 and 140 Ry to represent the single-particle wave functions and charge density, respectively. The QDs were placed in a periodically repeated supercell, with the nearest distance between replica larger than 12 Å. Geometry relaxations were performed until forces acting on all atoms were smaller than 10^{-4} a.u. For each dot, we assumed a cubic β -SiC core structure and we considered six different surface geometries: three different terminations (C, Si, or Si-rich), and two different surface structures, i.e., ideally terminated or reconstructed (100) facets (with dimer formation). In the case of dots large enough to accommodate more complex reconstructions (i.e., with radius larger than 1.1 nm), we also considered a (3×1)-like reconstruction¹⁷ of (100) facets. For each cluster, after preparing the initial core cubic geometry with a surface reconstructed in a manner similar to the bulk, we fully optimized all atomic coordinates using damped molecular dynamics or conjugate gradient algorithms. More details about the dot geometry optimization will be given elsewhere.

In Figure 1 we report the electronic gap obtained for several SiC clusters with different terminations as the difference between the lowest unoccupied molecular orbital (LUMO) and the highest occupied molecular orbital (HOMO) eigenvalues. Previous work on Si and C has shown^{18–20} that the HOMO–LUMO energy difference underestimates the optical gap of QDs (e.g., by about 1.5 eV in Si), as compared with more accurate methods such as quantum Monte Carlo (QMC). However, HOMO–LUMO and QMC gaps have

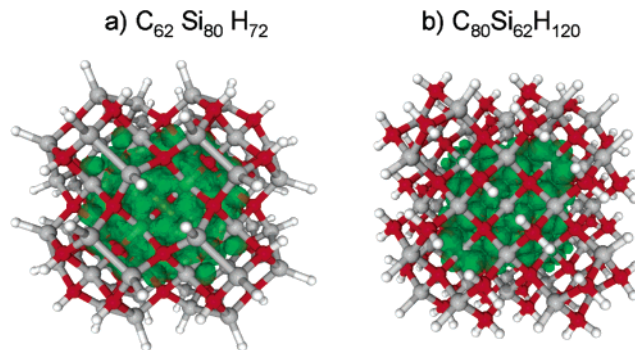


Figure 2. (Color) Ball and stick model of two SiC quantum dots with the same shape and radius (1.13 nm, see Figure 1) but with different surface termination and reconstruction: (a) $C_{62}Si_{80}H_{72}$ with a (2×1) Si-terminated surface; (b) $C_{80}Si_{62}H_{120}$ with a (1×1) C-terminated surface. Red (gray) spheres represent C (Si) atoms; white spheres represent H atoms. The green three-dimensional isosurface encloses 95% of the probability densities of the LUMO state for each dot. In both cases the LUMO is mostly localized within the dot core.

been shown to provide the same qualitative trend as a function of the nanoparticle size and surface structure. Therefore, here we refer to the “energy gap” or “gap” of the SiC nanoparticle as the HOMO–LUMO energy difference, and we expect the computed values to be shifted roughly by 1–2 eV in QMC calculations for each surface composition.

It is clear from Figure 1 that, though in general the gap increases as the size of the SiC QDs is reduced, the structure of the surface has a dominant role. The difference in the nanoparticle gap as a function of the surface structure, at fixed size, is comparable to the difference due to the size reduction by 1 nm. In general, C-terminated and H-rich QDs have the largest gap, and for diameter of about 2.5 nm, they are expected to be UV emitter (after the QMC correction is taken into account). The small C-terminated SiC QDs have a gap comparable to or larger than diamond QDs with the same number of atoms.²¹ However, if the surfaces are Si-terminated or H-poor, the gaps of SiC QDs systematically decrease. For example, (1×1)-Si-terminated clusters exhibit smaller gaps than the (1×1)-C-terminated ones. With even smaller gaps come the cases of (2×1) reconstructed Si or C clusters. In the C case, the formation of surface dimers not only reduces the gap but also makes it almost size independent in the 1–3 nm range. Irrespective of size, the C–C bonds of these surface dimers are highly stretched, and their geometrical arrangement is most probably the reason for the weak size dependence of the gap of reconstructed, C-terminated dots. Finally, the smallest gaps correspond to Si-terminated and Si rich dots; these gaps are as small as those of reconstructed pure Si dots.²² The gaps of Si rich SiC-QDs are weakly dependent on hydrogen content.

There is a single size of nanoparticles whose optical gaps seem to depart from the general trends identified above. This is the case of $C_xSi_yH_z$, where $x = (62 \text{ or } 80)$, $y = (142 - x)$, and $z = (120, 108, \text{ or } 72)$. Here, reconstruction effects are amplified because the ideal geometry corresponds to an almost perfect cube with six relatively large (100) facets (see Figure 2). On a Si-terminated (1×1)-cluster, such as C_{62} -

Si₈₀H₁₂₀, the (100) facets are so large that the distortions induced by the H–H steric repulsion are stronger than in the other members of the Si-terminated (1×1) family.

Our calculations indicate that the differences in optical gaps discussed above come from differences in structural properties of the dots, not only at the surface but also in the bond lengths of the nanoparticle core. To illustrate this point, we show in Figure 2 the atomic geometry of (2×1)-like Si-terminated C₆₂Si₈₀H₇₂ (a) and (1×1)-like C-terminated C₈₀Si₆₂H₁₂₀ (b), together with the isosurface that encloses 95% of the square modulus of the LUMO wave function. These are dots with similar sizes (1.13 nm) and they are examples of the most stable surface geometries at equilibrium (see below). In both cases, 95% of the wave function is confined in the core of the QD, contrary to the case of reconstructed Si dots where the LUMO is mostly concentrated at the surface.¹⁹ A similar behavior is observed for the HOMOs (not shown). While the LUMO localization is slightly different in C₆₂Si₈₀H₇₂ and C₈₀Si₆₂H₁₂₀, this difference is too small to explain the large differences in the HOMO–LUMO gaps in the two cases (0.43 eV) [see Figure 1]. It turns out that in C₈₀Si₆₂H₁₂₀, first neighbor Si–C distances are expanded by 5% as compared to C₆₂Si₈₀H₇₂ and to the bulk lattice constant. In contrast, while there are some distortions in the first neighbor distances of C₆₂Si₈₀H₇₂ compared to the bulk, the overall volume is preserved as compared to the one obtained using a bulk lattice constant. The lattice expansion induced by CH₂ surface groups is most probably responsible for the large gaps obtained in the case of (1×1)-C-terminated dots.

We now turn to the discussion of the influence of surface reconstruction and stoichiometry on the relative stability of SiC dots. If the formation of SiC QDs is driven by kinetics, then in principle any of the surfaces previously discussed could be formed. However, if SiC QDs are formed at or near equilibrium conditions, only the geometries minimizing the free energy of the whole system would appear. To determine the preferred structure of SiC dots at equilibrium, we have computed the free energy (Ω) of SiC clusters as

$$\Omega = E_{\text{tot}} - TS - \mu_{\text{C}}N_{\text{C}} - \mu_{\text{Si}}N_{\text{Si}} - \mu_{\text{H}}N_{\text{H}} \quad (1)$$

where E_{tot} is the total formation energy obtained in our calculations, T is the temperature, S is the vibrational entropy, and μ_x and N_x are the chemical potential and number of atoms of element x (C, Si, or H) in the cluster. The entropy contribution is similar for clusters with the same size, and it is thus expected to be a minor correction to the value of Ω ; therefore, we assume that vibrational entropy differences are negligibly small. By choosing the lowest free energy structure for a given size, we have constructed a phase diagram in terms of $\delta\mu$ ($\delta\mu = \mu_{\text{Si}} - \mu_{\text{C}}$) and μ_{H} , which, in a high pressure^{23,24} or CVD⁸ growth from C_xSi_yH_z precursors, would correspond to specific concentration and temperature conditions. We find a phase diagram, summarized in Figure 3, which is basically independent of the size of the dot.

In Figure 3 the areas of constant color correspond to values of μ_{H} and $\delta\mu$ (which in turn correspond to concentration and

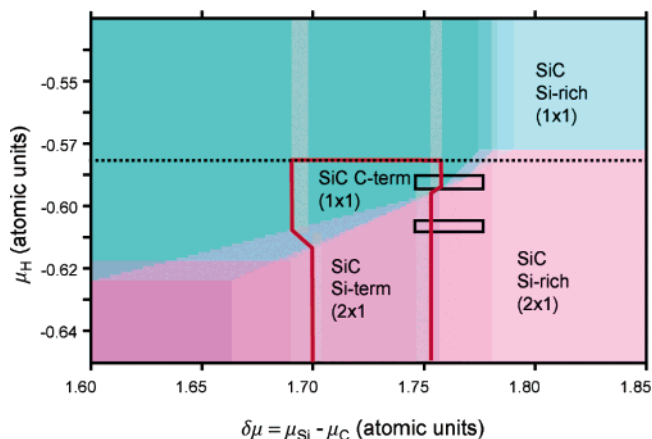


Figure 3. Relative stability of SiC dots with different surface structures as a function of the difference between the Si and C chemical potentials ($\delta\mu = \mu_{\text{Si}} - \mu_{\text{C}}$) and the hydrogen chemical potential (μ_{H}). The horizontal dotted line indicates the value of μ_{H} , above which SiC dissociates into silane and methane. The vertical gray thick lines denote transition regions where, depending on size and surface structure, SiC dots are not energetically favored as compared with either pure Si (left) or pure C dots (right). SiC QDs are stable within the area enclosed in red. The horizontal rectangles denote examples of values of $\delta\mu$ and μ_{H} that can be reached experimentally (see text).

T values), yielding the same minimum-energy SiC surface structure for all sizes. In the transition region between different colors, the curvature of the surface plays a role and the most stable surface structure does depend on the size of the QD. The horizontal dotted line indicates the value of μ_{H} , above which bulk β -SiC would spontaneously dissociate into CH₄ and SiH₄. The thick vertical bars on the right (left) hand side of Figure 3 correspond to the size and surface dependent transition region where the value of $\delta\mu$ is so high (low) that pure Si (C) QDs become more stable than SiC QDs. The region highlighted in red corresponds to the stability region of SiC dots, with the most stable structures being (1×1) C-terminated and (2×1) Si-terminated.

An important result emerging from Figure 3 is that synthesis of thermodynamically stable, hydrogenated SiC dots will lead only to two specific types of nanoparticles: either dots with (1×1) C-terminated surfaces or dots with (2×1)-reconstructed Si-terminated surfaces. As discussed above (see Figure 1), for the same core size, these two surface terminations give rise to very different gaps. From Figure 3 we see that, for example, (1×1) Si-terminated and Si-rich clusters would never form at equilibrium because their formation would require (i) $\delta\mu$ being so large that (1×1) pure Si QDs would have lower energy than SiC dots and (ii) μ_{H} being so high that the β -SiC lattice would evaporate into CH₄ and SiH₄. For these large values of $\delta\mu$, (2×1)-like Si rich clusters are also metastable as compared to pure Si QD. For low values of $\delta\mu$ we find that (2×1) C-terminated clusters have higher energy than pure C QDs.

We notice that in our study we have considered only surfaces without defects. But our results suggest that in the transition regions from one stable phase to another, defect formation would cost very little energy. For example, Si-rich (2×1) reconstructed facets on SiC QDs would require

a small amount of energy to form in the Si/SiC transition region of the phase diagram. This type of defect would give gaps comparable to the ones of small pure Si dots.

It is interesting to discuss our findings about the relative stability of Si and SiC dots in connection with recent high-pressure (P) experiments reporting the formation of Si nanoparticles.^{23,24} In particular, we consider the upper horizontal black rectangle of Figure 3, which corresponds to values of the chemical potential accessible in a high P experiment at approximately 300 atm, where the partial pressure of hydrogen [H₂] ranges from 95% to 5%, the [CH₄]/[SiH₄] ratio is between 10² and 10⁻², and T is fixed at 800 K. The lower horizontal rectangle of the figure corresponds to similar T and gas concentration conditions, but P = 3 atm. These results show that, consistent with experiment, under some of the conditions reported in refs 23 and 24, Si QDs are more stable than SiC dots, and thus are more likely to form. However, as the [CH₄]/[SiH₄] ratio grows above 10, $\delta\mu$ decreases and eventually the formation of SiC dots is favored over that of Si dots, with the smallest (1 nm) SiC QD expected to form before the larger ones. For higher [CH₄]/[SiH₄] ratios and high P, C-terminated (1 × 1) quantum dots would form, while at low pressures Si-terminated (2 × 1) would be more stable. We note that the conditions of high-P experiments reported in refs 23 and 24 are very close to those leading to the formation of SiC quantum dots and that there are values of the [CH₄]/[SiH₄] ratio where it is possible to form large Si QDs and small SiC QDs at the same time. The small SiC dots with surface defects might be responsible for blue luminescence.

In summary, we have presented a series of ab initio calculations of the structural and electronic properties of SiC dots with 1 to 3 nm diameter. Our results show that surface structure and composition play a dominant role in determining both the stability and the optical gaps of these nanoparticles. In particular, we have found that size and surface composition of SiC dots can be engineered to obtain absorption and emission from the UV to the green. Based on our results, we have proposed that small SiC nanoparticles are good candidates to build nanostructured materials for semiconductor-based UV light sources. Finally, we have discussed our findings on the relative stability of SiC and Si dots in connection with recent high-pressure Si synthesis experiments; we have proposed that under certain experimental conditions both SiC and Si dots may be formed and that the small SiC dots may be the ones responsible for blue emission.

Acknowledgment. We thank F. Gygi for providing the GP code and for useful discussions. This work was performed under the auspices of the U.S. Department of Energy at the University of California/Lawrence Livermore National Laboratory under contract no. W-7405-Eng-48.

References

- (1) Zhang, P.; Crespi, V.; Chang, E.; Louie, S. G.; Cohen, M. L. *Nature* **2001**, *409*, 69.
- (2) Martin, R. M. *Electronic Structure: Basic Theory and Practical Methods*; Cambridge University Press: Cambridge, 2004.
- (3) Pascoli, G.; Lavendy, H. *Int. J. Mass Spectrom.* **1998**, *177*, 31.
- (4) Tsuruta, K.; Totsuji, H.; Totsuji, C. *Mater. Transac.* **2001**, *42*, 2261.
- (5) Xu, S. J.; Yu, M. B.; Rusli; Yoom, S. M.; Che, C. M. *Appl. Phys. Lett.* **2000**, *76*, 2550.
- (6) Zhao, J.; Mao, D. S.; Lin, Z. X.; Jiang, B. Y.; Yu, Y. H.; Liu, X. H.; Wang, H. Z.; Yang, G. Q. *Appl. Phys. Lett.* **1998**, *73*, 1838.
- (7) Li, X.; Shao, C.; Qiu, S.; Xiao, F.-S.; Zheng, W.; Liu, Z.; Terasaki, O. *Mater. Lett.* **2001**, *48*, 242.
- (8) Huang, Z. R.; Liang, B.; Jiang, D. L.; Tan, S. H. *J. Mater. Sci.* **1996**, *4227*.
- (9) Huisken, F.; Kohn, B.; Alexandrescu, R.; Cojocaru, S.; Crunteanu, A.; Ledoux, G.; Reynaud, C. *J. Nanoparticle Res.* **1999**, *1*, 293.
- (10) Takazawa, A.; Tamura, T.; Yamada, M. *Jpn. J. Appl. Phys.* **1993**, *32*, 3148.
- (11) Shor, J. S.; Bermis, L.; Kurtz, A. D.; Grimber, I.; Weiss, B.-Z.; MacMillan, M. F.; Choyke, W. J. *J. Appl. Phys.* **1994**, *76*, 4045.
- (12) Matsumoto, T.; Takahashi, J.; Tamaki, T.; Futagi, T.; Mimura, H. *Appl. Phys. Lett.* **1994**, *64*, 226.
- (13) Petrova-Koch, V.; Sreseli, O.; Polisski, G.; Kovalev, D.; Muschik, T.; Koch, F. *Thin Solid Films* **1995**, *255*, 107.
- (14) Perdew, J. P.; Burke, K.; Ernzerhof, M. *Phys. Rev. Lett.* **1996**, *77*, 3865, 3868.
- (15) Gygi, F. *The GP Code*; LLNL, 2002.
- (16) Troullier, N.; Martins, J. L. *Phys. Rev. B* **1991**, *43*, 1993, 2006.
- (17) Chabal, Y. J.; Raghavachari, K. *Phys. Rev. Lett.* **1985**, *54*, 1055, and references therein.
- (18) Williamson, A.; Grossman, J.; Hood, R.; Puzder, A.; Galli, G. *Phys. Rev. Lett.* **2002**, *89*, 196803.
- (19) Puzder, A.; Williamson, A. J.; Reboredo, F. A.; Galli, G. *Phys. Rev. Lett.* **2003**, *91*, 157405.
- (20) Drummond, N.; Williamson, A. J.; Needs, R.; Galli, G., 2003, private communication.
- (21) The gap of Si₁₃C₁₆H₃₆ (-5.615 eV) is similar to the gap of C₂₉H₃₆ (-5.594 eV) and the gap of Si₂₈C₃₈H₆₄ (-5.482 eV) is larger than that of C₆₆H₆₄ (-4.827 eV).
- (22) The gap of Si₂₅C₄H₂₄ is -4.924 eV, which is similar to the gap of Si₂₉H₂₄ (-4.969 eV). The gap of Si₅₂C₁₄H₄₀ (-4.219 eV) is also similar to that of Si₆₆H₄₀ (-4.659 eV).
- (23) Holmes, J. D.; Ziegler, K. J.; Doty, R. C.; Pell, L. E.; Johnston, K. P.; Korgel, B. *J. Am. Chem. Soc.* **2001**, *123*, 3748.
- (24) English, D. E.; Pell, L. E.; Yu, Z.; Barbara, P. F.; Korgel, B. A. *Nano Lett.* **2002**, *2*, 681.

NL049876K